



**NAVAL  
POSTGRADUATE  
SCHOOL**

**MONTEREY, CALIFORNIA**

**THESIS**

**CALCULATION OF THE TRANSITION MATRIX FOR THE  
SCATTERING OF ACOUSTIC WAVES FROM A THIN  
ELASTIC SPHERICAL SHELL USING THE COMSOL  
MULTIPHYSICS FINITE-ELEMENT CODE**

by

Kiang Chuan, Ng

December 2011

Thesis Co-Advisors:

Steve Baker  
Clyde L. Scandrett

**Approved for public release; distribution is unlimited**

THIS PAGE INTENTIONALLY LEFT BLANK

REPORT DOCUMENTATION PAGE			Form Approved OMB No. 0704-0188	
Public reporting burden for this collection of information is estimated to average 1 hour per response, including the time for reviewing instruction, searching existing data sources, gathering and maintaining the data needed, and completing and reviewing the collection of information. Send comments regarding this burden estimate or any other aspect of this collection of information, including suggestions for reducing this burden, to Washington headquarters Services, Directorate for Information Operations and Reports, 1215 Jefferson Davis Highway, Suite 1204, Arlington, VA 22202-4302, and to the Office of Management and Budget, Paperwork Reduction Project (0704-0188) Washington DC 20503.				
1. AGENCY USE ONLY (Leave blank)		2. REPORT DATE December 2011	3. REPORT TYPE AND DATES COVERED Master's Thesis	
4. TITLE AND SUBTITLE Calculation of the Transition Matrix for the Scattering of Acoustic Waves from a Thin Elastic Spherical Shell Using the COMSOL Multiphysics Finite-Element Code			5. FUNDING NUMBERS	
6. AUTHOR(S) Kiang Chuan, Ng				
7. PERFORMING ORGANIZATION NAME(S) AND ADDRESS(ES) Naval Postgraduate School Monterey, CA 93943-5000			8. PERFORMING ORGANIZATION REPORT NUMBER	
9. SPONSORING /MONITORING AGENCY NAME(S) AND ADDRESS(ES) N/A			10. SPONSORING/MONITORING AGENCY REPORT NUMBER	
11. SUPPLEMENTARY NOTES The views expressed in this thesis are those of the author and do not reflect the official policy or position of the Department of Defense or the U.S. Government. IRB Protocol number _____N/A_____.				
12a. DISTRIBUTION / AVAILABILITY STATEMENT Approved for public release; distribution is unlimited			12b. DISTRIBUTION CODE A	
13. ABSTRACT (maximum 200 words) In acoustics, the so-called Transition, or T-matrix relates the incident and scattered acoustic pressures of an object or scatterer. The T-matrix of a thin steel spherical shell in water has been determined by the COMSOL Multiphysics Finite-Element Code. The shell has an outer radius of 0.5m and a thickness of 1cm. It is driven at a frequency of 474 Hz such that $ka=1$ (where $k$ is the acoustic wave number and $a$ is the outer radius of the shell). A standing wave, represented by a spherical Bessel function, is incident onto the shell surface and the corresponding scattering coefficient is computed. The approach is divided into three portions. Firstly, a fluid-loaded rigid sphere is modeled using the Acoustic-Shell Interaction (ACSH) physics mode to examine the functionality of COMSOL. It also explores the degree of improvement when a refined fluid mesh is applied. Secondly, a thin spherical shell is modeled in the ACSH physics mode. This will examine the credibility of COMSOL to obtain accurate results based on thin shell approximation. Finally, a true 3D finite element, employing the 3D elastic theory, is created using the Acoustic-Structure Interaction (ACSI) physics mode. The resulting diagonal T-matrix elements achieved an accuracy of 0.1% relative to the analytical T-matrix. Ultimately, these results will be applicable to the modeling of the radiation from an arbitrarily densely-packed array of sonar transducers.				
14. SUBJECT TERMS Type Keywords Here			15. NUMBER OF PAGES 53	
			16. PRICE CODE	
17. SECURITY CLASSIFICATION OF REPORT Unclassified	18. SECURITY CLASSIFICATION OF THIS PAGE Unclassified	19. SECURITY CLASSIFICATION OF ABSTRACT Unclassified	20. LIMITATION OF ABSTRACT UU	

THIS PAGE INTENTIONALLY LEFT BLANK

**Approved for public release; distribution is unlimited**

**CALCULATION OF THE TRANSITION MATRIX FOR THE SCATTERING OF  
ACOUSTIC WAVES FROM A THIN ELASTIC SPHERICAL SHELL USING  
THE COMSOL MULTIPHYSICS FINITE-ELEMENT CODE**

Kiang Chuan, Ng  
Major, Singapore Armed Forces  
B.E., University of Queensland, 2005

Submitted in partial fulfillment of the  
requirements for the degree of

**MASTER OF SCIENCE IN COMBAT SYSTEMS TECHNOLOGY**

from the

**NAVAL POSTGRADUATE SCHOOL  
Dec 2011**

Author: Kiang Chuan, Ng

Approved by: Steve Baker  
Thesis Co-Advisor

Clyde L. Scandrett  
Thesis Co-Advisor

Larraza, Andres  
Chair, Department of Physics

THIS PAGE INTENTIONALLY LEFT BLANK

## ABSTRACT

In acoustics, the so-called Transition, or T-matrix relates the incident and scattered acoustic pressures of an object or scatterer. The T-matrix of a thin steel spherical shell in water has been determined by the COMSOL Multiphysics Finite-Element Code. The shell has an outer radius of 0.5m and a thickness of 1cm. It is driven at a frequency of 474 Hz such that  $ka=1$  (where  $k$  is the acoustic wave number and  $a$  is the outer radius of the shell). A standing wave, represented by a spherical Bessel function, is incident onto the shell surface and the corresponding scattering coefficient is computed. The approach is divided into three portions. Firstly, a fluid-loaded rigid sphere is modeled using the Acoustic-Shell Interaction (ACSH) physics mode to examine the functionality of COMSOL. It also explores the degree of improvement when a refined fluid mesh is applied. Secondly, a thin spherical shell is modeled in the ACSH physics mode. This will examine the credibility of COMSOL to obtain accurate results based on thin shell approximation. Finally, a true 3D finite element, employing the 3D elastic theory, is created using the Acoustic-Structure Interaction (ACSI) physics mode. The resulting diagonal T-matrix elements achieved an accuracy of 0.1% relative to the analytical T-matrix. Ultimately, these results will be applicable to the modeling of the radiation from an arbitrarily densely-packed array of sonar transducers.

THIS PAGE INTENTIONALLY LEFT BLANK

# TABLE OF CONTENTS

<b>I.</b>	<b>INTRODUCTION.....</b>	<b>1</b>
<b>A.</b>	<b>BACKGROUND .....</b>	<b>1</b>
<b>B.</b>	<b>PURPOSE.....</b>	<b>1</b>
<b>C.</b>	<b>THESIS OUTLINE.....</b>	<b>2</b>
<b>II.</b>	<b>THEORY .....</b>	<b>3</b>
<b>A.</b>	<b>THE “T-MATRIX” APPROACH.....</b>	<b>3</b>
1.	Single Transducer .....	3
2.	Array of Transducers .....	4
<b>B.</b>	<b>FORCED VIBRATION OF A THIN SPHERICAL SHELL .....</b>	<b>6</b>
<b>III.</b>	<b>COMSOL MULTIPHYSICS FINITE-ELEMENT CODE .....</b>	<b>11</b>
<b>A.</b>	<b>INTRODUCTION TO COMSOL ACOUSTIC MODULE.....</b>	<b>11</b>
1.	Acoustic-Structure Interaction Physics Mode.....	11
2.	Acoustic-Shell Interaction Physics Mode.....	12
<b>B.</b>	<b>THE 3D MODEL .....</b>	<b>13</b>
1.	Model Parameters.....	13
2.	Radiation boundary .....	14
3.	Meshing.....	14
4.	Incident wave onto shell surface.....	15
<b>C.</b>	<b>COMSOL MODELING FOR T-MATRIX DETERMINATION.....</b>	<b>15</b>
<b>IV.</b>	<b>RESULTS .....</b>	<b>19</b>
<b>A.</b>	<b>T-MATRIX OF A RIGID SPHERE IN FLUID.....</b>	<b>19</b>
<b>B.</b>	<b>T-MATRIX OF A THIN SPHERICAL SHELL USING THIN SHELL APPROXIMATION.....</b>	<b>22</b>
1.	Analytical T-matrix .....	22
2.	COMSOL Results for Thin Shell Approximation Modeling .....	22
a.	<i>Diagonal elements of T-matrix.....</i>	<i>22</i>
b.	<i>Non-diagonal elements of T-matrix .....</i>	<i>24</i>
c.	<i>Evaluation of T-matrix within fluid (at radius = 1m and 2m).....</i>	<i>26</i>
<b>C.</b>	<b>T-MATRIX OF A THIN SPHERICAL SHELL USING 3D ELASTIC THEORY .....</b>	<b>26</b>
1.	Analytical T-matrix .....	27
2.	COMSOL Results for 3D Elastic Shell Modeling .....	27
a.	<i>Diagonal elements of T-matrix.....</i>	<i>27</i>
b.	<i>Non-diagonal elements of T-matrix .....</i>	<i>29</i>
<b>V.</b>	<b>CONCLUSIONS AND FUTURE WORK.....</b>	<b>31</b>
<b>A.</b>	<b>CONCLUSIONS .....</b>	<b>31</b>
<b>B.</b>	<b>FUTURE WORK.....</b>	<b>32</b>
1.	External determination of scattering coefficients .....	32
2.	Perform swept mesh in radial direction.....	32

3. Perfectly Matched Layer (PML) .....	33
LIST OF REFERENCES.....	35
INITIAL DISTRIBUTION LIST .....	37

## LIST OF FIGURES

Figure 1.	Interaction between an array of two transducer (From Ruiz, 1994) [2] .....	5
Figure 2.	Array of 16 closely packed spherical shell transducer (From Baker, 1998) [1].....	6
Figure 3.	(a) Spherical coordinates. After [5]. (b) Displacement components u, v and w.....	7
Figure 4.	3D Model of a thin spherical shell submerged in fluid.....	13
Figure 5.	Model with finer mesh for the fluid domain and extremely fine mesh for the thin shell.....	15
Figure 6.	Workflow of COMSOL Modeling.....	16

THIS PAGE INTENTIONALLY LEFT BLANK

## LIST OF TABLES

Table 1.	Analytical T-matrix for a rigid sphere .....	20
Table 2.	COMSOL: T-matrix for a rigid sphere .....	21
Table 3.	Analytical T-matrix for a thin shell at $n=0, 1$ and $2$ .....	22
Table 4.	COMSOL: Diagonal T-matrix elements for a thin shell (fluid domain: extra fine meshes and shell surface: extremely fine meshes) .....	23
Table 5.	ATILA: Diagonal T-matrix elements for a thin shell [2, Chp 3].....	24
Table 6.	Non-diagonal elements in the T-matrix normalized to diagonal element in the same column (Thin shell approximation) .....	25
Table 7.	COMSOL: Diagonal T-matrix elements at radius = 1m and 2m respectively (fluid domain: extra fine meshes and shell surface: extremely fine meshes) .....	26
Table 8.	Analytical T-matrix for a thin shell using 3D elastic theory .....	27
Table 9.	COMSOL: Diagonal T-matrix elements for a thin shell using 3D elastic theory (fluid domain: finer meshes and shell: coarser meshes).....	28
Table 10.	Improved meshing for computing $R_{00}$ using 3D elastic theory (fluid: finer meshes and solid: finer meshes) .....	29
Table 11.	Non-diagonal elements in the T-matrix normalized to diagonal element in the same column (3D Elastic Theory) .....	30

THIS PAGE INTENTIONALLY LEFT BLANK

## **ACKNOWLEDGMENTS**

I would like to thank my thesis advisor, Professor Steve Baker, for his guidance and endless patience in enriching my knowledge for the thesis. I appreciate the time and effort he had spent to supervise the analysis work involved in the thesis.

I would also like to thank my second thesis advisor, Professor Clyde Scandrett, for his professional inputs and promptness to my queries.

I am grateful to Mr John Dunec from COMSOL, for his valuable consultations which raised my confidence in the modeling.

Last but not least, I want to thank my wife, Gina, for her support and her good care for my son, Remus, when I was occupied with my studies.

THIS PAGE INTENTIONALLY LEFT BLANK

# I. INTRODUCTION

## A. BACKGROUND

In the purview of underwater naval operations, accurate target detection motivates the need to deploy active sonar arrays. Understanding the interactions among the elements of an array of sonar transducers is critical. Due to the fact that each transducer radiates in close proximity to one another, mutual interference occurs. The technique employed in common practice to model this array element interaction [9, Chp 8] is not applicable when the array elements are closely-packed. This led to the emergence of a research program to develop the so-called Transition, or T-matrix method for modeling the radiation from an arbitrarily densely-packed array of sonar transducers [1, 3].

The T-matrix relates the incident pressure applied on a particular transducer to its scattered pressure at a specific harmonic component. The scattering properties can be determined through Finite Element Modeling (FEM), where a known pressure field is imposed on the transducer, in this case, represented by a thin spherical shell. The T-matrix of a single transducer will subsequently be incorporated into the calculation of the scattered pressures from an array of sonar transducers.

The analytical T-matrix can be determined from the modal mechanical impedance of a spherical shell, which relates the pressures and the displacement components. These analytical values form the basis for validation of the modeled results. In a previous attempt using the ATILA finite-element code, the computed T-matrix was deemed unsatisfactory in some aspects [2]. The discrepancies could be due to the ineffectiveness of the radiation boundary condition and the coarse mesh built for the model.

## B. PURPOSE

This thesis investigates the use of COMSOL Multiphysics finite-element code for the computation of the T-matrix for a thin spherical shell. A 3D model of a water-loaded spherical thin steel shell with an outer radius of 0.5m and a thickness of 1cm was

constructed, employing several fine meshes. The scattering T-matrix elements for this shell were computed at a frequency of 474 Hz (i.e.,  $ka=1$ ). Two acoustic-structure interaction types of models were created, one employing 2-D thin shell elements to model the physical shell and one in which 3-D elastic elements were used to model the physical shell.

In the model calculations, an incident wave distributed in angle as one spherical harmonic component was applied and the corresponding scattered waves, in terms of the spherical harmonic components, were evaluated. Scattering coefficients for the zero (monopole), first (dipole) and second (quadrupole) order modes were determined. The computed T-matrix was validated with reference to analytical values.

### **C. THESIS OUTLINE**

The subsequent chapters of the thesis are outlined as follows:

- Chapter II covers two parts of the theory. The first part entails the T-matrix theory involving the necessary equations that lead to the formulation for a single transducer and an array of transducers. The second part illustrates the theory of forced vibration of a spherical shell and a series of manipulations used to derive the analytical T-matrix.
- Chapter III introduces the features in the COMSOL Multiphysics Finite-Element code and presents the 3D model of the water-loaded thin spherical shell.
- Chapter IV presents the T-matrix results determined by COMSOL modeling and the percentage of error with respect to the analytical values.
- Chapter V presents the conclusions of the thesis and suggestions for future work.

## II. THEORY

### A. THE “T-MATRIX” APPROACH

The “T-matrix” relates the incident and scattered waves from an obstacle or scatterer. From the free-field radiation and (short-circuit) scattering properties of a single active sonar transducer, as represented in the T-matrix, one can compute the radiation properties of an array of arbitrarily densely and randomly packed sonar transducers [1]. The relationship between the incident pressure,  $P^i$ , and the scattered pressure,  $P^s$ , on a single element is represented by:

$$\{P^s\} = [T]\{P^i\} \quad (1)$$

where  $\{ \}$  represents a column of coefficients and  $[T]$  is the T-matrix.

#### 1. Single Transducer

For a particular transducer submerged in fluid, an incident wave is represented by a standing spherical wave. It is comprised of a discrete basis set of (unnormalized) spherical harmonics, with an  $e^{i\omega t}$  harmonic time dependence assumed, and is expressed in the form of:

$$P^i(r, \theta, \phi) = \sum_{n=0}^{\infty} \sum_{m=-n}^n P_{nm}^i j_n(kr) P_n^m(\cos \theta) e^{im\phi} \quad (2)$$

The scattered pressure is similarly represented by:

$$P^s(r, \theta, \phi) = \sum_{n=0}^{\infty} \sum_{m=-n}^n P_{nm}^s h_n^{(2)}(kr) P_n^m(\cos \theta) e^{im\phi} \quad (3)$$

where:

- $n, m, \theta, \phi$  : spherical harmonics indices of arguments
- $P_{nm}^i$  : coefficient of the incident pressure
- $j_n(kr)$  :  $n^{\text{th}}$  order spherical Bessel function of the first kind

$P_n^m(\cos \theta)$  : associated Legendre function of the first kind

$h_n^{(2)}$  :  $n^{\text{th}}$  order spherical Hankel function of the second kind

## 2. Array of Transducers

In an array of active transducers, where their mutual field interactions are to be taken into account, the T-matrix formulation will have to involve the use of the spherical addition theorem. Considering an array of two transducers, illustrated in Figure 1 [2, Chp 2], whereby their radiated fields interact with each other, the formulation is as follows:

$$T_1 G_{12}(\overline{A}_2 + \overline{B}_2) = \overline{A}_1 \quad (4)$$

$$T_2 G_{21}(\overline{A}_1 + \overline{B}_1) = \overline{A}_2 \quad (5)$$

where:

$G_{ij}$  : translation formula from system  $j$  to system  $i$   
(by the spherical addition formula)

$T_k$  : T-matrix for the  $k^{\text{th}}$  transducer modeled

$\overline{B}_1$  and  $\overline{B}_2$  : radiated amplitudes of the two transducers

$\overline{A}_1$  and  $\overline{A}_2$  : scattering pressure amplitudes of the two transducers

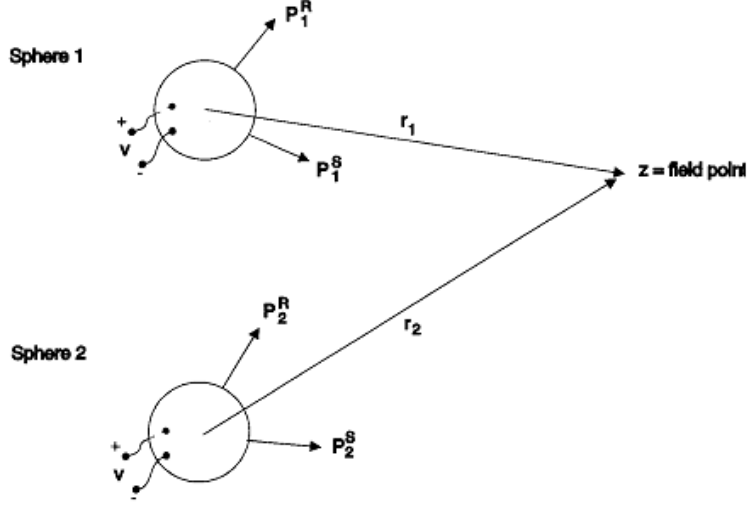


Figure 1. Interaction between an array of two transducer (From Ruiz, 1994) [2]

Putting into matrix form:

$$\begin{pmatrix} \mathbf{I} & -\mathbf{T}_1\mathbf{G}_{12} \\ -\mathbf{T}_2\mathbf{G}_{21} & \mathbf{I} \end{pmatrix} \begin{pmatrix} \overline{\mathbf{A}}_1 \\ \overline{\mathbf{A}}_2 \end{pmatrix} = \begin{pmatrix} \mathbf{T}_1\mathbf{G}_{12}\overline{\mathbf{B}}_2 \\ \mathbf{T}_2\mathbf{G}_{21}\overline{\mathbf{B}}_1 \end{pmatrix} \quad (6)$$

After simplification, the resulting equation becomes:

$$(\mathbf{I} - \partial) \begin{pmatrix} \overline{\mathbf{A}}_1 \\ \overline{\mathbf{A}}_2 \end{pmatrix} = \partial \begin{pmatrix} \overline{\mathbf{B}}_1 \\ \overline{\mathbf{B}}_2 \end{pmatrix} \quad (7)$$

where:

$$\partial = \begin{pmatrix} 0 & \mathbf{T}_1\mathbf{G}_{12} \\ \mathbf{T}_2\mathbf{G}_{21} & 0 \end{pmatrix} \quad (8)$$

Upon the determination of  $\overline{\mathbf{A}}_1$  and  $\overline{\mathbf{A}}_2$ , the total pressure at any field point can be obtained by summation over the entire array element:

$$P(r, \theta, \phi) = \sum_j \sum_{n=0}^N \sum_{m=-n}^n [A_{jmn} + B_{jmn}] h_n(kr_j) P_n^m(\cos \theta) e^{im\phi} \quad (9)$$

As an example, this methodology enables the determination of the source levels for an array of 16 closely packed spherical shell transducers operating at 474Hz ( $ka=1$ ) as shown in Figure 2 [1]:

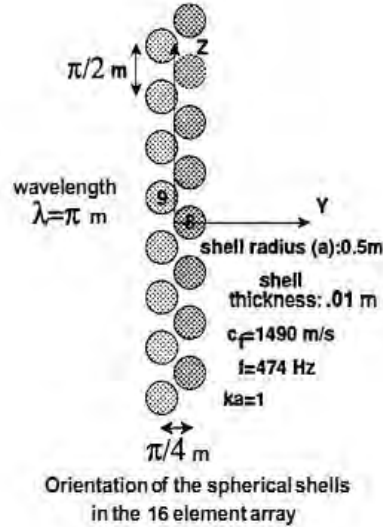


Figure 2. Array of 16 closely packed spherical shell transducer (From Baker, 1998) [1]

## B. FORCED VIBRATION OF A THIN SPHERICAL SHELL

We follow the analysis by Junger and Feit of the forced vibration of a thin spherical shell [4, Chp 7]. In the study of acoustic-structure interaction problem, they adopted Loves's assumptions for the equations of motion of thin elastic shells:

- The thickness of a shell is small compared with the smallest radius of the curvature of the shell.
- The displacement is small in comparison with the shell thickness.
- The transverse normal stress acting on planes parallel to the shell middle surface is negligible.
- Fibers of the shell normal to the middle surface remain so after deformation and are themselves not subject to elongation.

In addition, the shell is thin enough and the frequency low enough to ignore flexural stresses as compared with membrane stresses [4, Chp 11].

As a result, the displacements of the spherical shell can be perceived as a function of the shell's middle surface deflection, shown in Figure 3 [5].

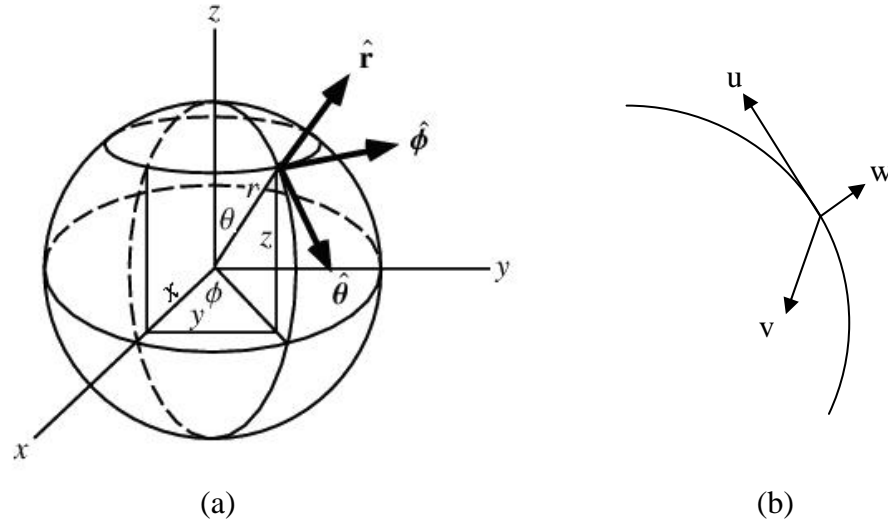


Figure 3. (a) Spherical coordinates. After [5]. (b) Displacement components u, v and w

In view of nontorsional axisymmetric motions of a spherical shell, the tangential component vanishes in  $\phi$ , the azimuthal direction. The existing components are w, the mid-surface radial motion and u, the tangential motion in the direction of increasing  $\theta$ , and both are independent of  $\phi$ . A further optimization [2, Chp 2] reduced the equation to contain only the w component. The resulting equation of interest is, therefore, the modal mechanical impedance, given by [4, Chp 7]:

$$Z_n = \frac{F_{nm}}{i\omega w_{nm}} \quad (10)$$

where  $F_{nm}$  is the normal force per unit area directed radially outward, and represents the sum of the incident and outgoing spherical wave in the form:

$$F_{nm} = - \left\{ \underbrace{j_n(ka)I_{nm}}_{\text{Incident}} + \underbrace{h_n^{(2)}(ka)R_{nm}}_{\text{Outgoing}} \right\} \quad (11)$$

The respective incident pressure, scattered pressure and radial displacement can be expressed as:

$$p^i = \sum_{nm} I_{nm} j_n(kr) P_n^m(\cos \theta) e^{im\phi} \quad (12)$$

$$p^s = \sum_{nm} R_{nm} h_n^{(2)}(kr) P_n^m(\cos \theta) e^{im\phi} \quad (13)$$

$$w = \sum_{nm} w_{nm} P_n^m(\cos \theta) e^{im\phi} \quad (14)$$

where  $I_{nm}$  and  $R_{nm}$  are the incident and reflected modal amplitudes respectively, and  $w_{nm}$  is the modal normal displacement of the shell. The pressure at the shell surface is:

$$p = p^i + p^s \quad (15)$$

Expressing the modal mechanical impedance as [4, Chp 7]:

$$Z_n = i \frac{h C_p \rho_s}{a \Omega} \left\{ \frac{[\Omega^2 - 2(1+\nu)](\Omega^2 + 1 - \nu - \lambda_n) - \lambda_n (1+\nu)^2}{\Omega^2 + 1 - \nu - \lambda_n} \right\} \quad (16)$$

where

$$\lambda_n = n(n+1)$$

$$\Omega = \frac{\omega a}{C_p}$$

- $\omega$  : angular frequency
- $h$  : shell thickness
- $C_p$  : plate phase velocity
- $\nu$  : Poisson's ratio
- $E$  : Young's modulus
- $\rho_s$  : shell density
- $a$  : shell radius

Arranging Equations (10) and (11) yields:

$$I_{nm} j_n(ka) + R_{nm} h_n^{(2)}(ka) = -i\omega Z_n w_{nm} \quad (17)$$

Another relationship between  $I_{nm}$ ,  $R_{nm}$  and  $w_{nm}$  can be established using Euler's equation,

$$\frac{\partial p}{\partial r} \Big|_{r=a} = -\rho_f \frac{\partial^2 w}{\partial t^2} \Big|_{r=a} \quad (18)$$

where  $\rho_f$  is the density of the fluid, and with the assumption of no cavitation on the surface of the shell,

$$I_{nm} j_n'(ka) + R_{nm} h_n^{(2)'}(ka) = \omega \rho_f C_f w_{nm} \quad (19)$$

Eliminate  $w_{nm}$  by equating Equations (17) and (19), the relationship between  $I_{nm}$  and  $R_{nm}$  is simplified into:

$$R_{nm} = - \left\{ \frac{iZ_n j_n'(ka) + \rho_f C_f j_n(ka)}{iZ_n h_n^{(2)'}(ka) + \rho_f C_f h_n^{(2)}(ka)} \right\} I_{nm} \quad (20)$$

Equation (20) will be used to derive the analytical results of the T-matrix in which each value of  $R_{nm}$  corresponds to the diagonal element of the matrix when  $I_{nm}$  is set to one.

The T-matrix format for the harmonics up to the second order ( $n=2$ ) is as follows:

$$T = \begin{bmatrix} R_{00} & 0 & 0 & 0 & 0 & 0 & 0 & 0 & 0 \\ 0 & R_{1,-1} & 0 & 0 & 0 & 0 & 0 & 0 & 0 \\ 0 & 0 & R_{10} & 0 & 0 & 0 & 0 & 0 & 0 \\ 0 & 0 & 0 & R_{11} & 0 & 0 & 0 & 0 & 0 \\ 0 & 0 & 0 & 0 & R_{2,-2} & 0 & 0 & 0 & 0 \\ 0 & 0 & 0 & 0 & 0 & R_{2,-1} & 0 & 0 & 0 \\ 0 & 0 & 0 & 0 & 0 & 0 & R_{20} & 0 & 0 \\ 0 & 0 & 0 & 0 & 0 & 0 & 0 & R_{21} & 0 \\ 0 & 0 & 0 & 0 & 0 & 0 & 0 & 0 & R_{22} \end{bmatrix} \quad (21)$$

$\underbrace{\hspace{1.5cm}}$   
 Zero Order  
(Monopole)

$\underbrace{\hspace{2.5cm}}$   
 First Order  
(Dipole)

$\underbrace{\hspace{3.5cm}}$   
 Second Order  
(Quadrupole)

Due to spherical symmetric, the scattered wave should contain the same harmonic components as the incident wave. In other words, the resulting T-matrix should be diagonal and the non-diagonal values should be zero.

### **III. COMSOL MULTIPHYSICS FINITE-ELEMENT CODE**

This chapter introduces the useful features of the Acoustic Module in COMSOL Multiphysics [6] and describes the design of the 3D spherical thin shell model and its essential governing equations. For the purpose of achieving accurate results, the model simulation was attempted using two different “physics modes” - the Acoustic-Shell Interaction (ACSH) and the Acoustic-Structure Interaction (ACSI) modes. The key difference between these two physics modes is the theory that is governing the solid. The ACSH is governed by thin shell approximation whereas the ACSI employs the full 3D elastic theory. The rest of the chapter will cover the formulation of equations for the incident standing wave as well as the computation of the T-matrix elements with the resulting scattered pressure obtained in COMSOL.

#### **A. INTRODUCTION TO COMSOL ACOUSTIC MODULE**

The COMSOL Multiphysics Finite-Element Code is capable of solving real-time physics problem with precision. It contains a wide variety of modules for different “physics modes” that enables the user to define the conditions, physical effects and mathematical equations that are essential in the modeling. The Acoustic Module featured in COMSOL Multiphysics Version 4.2a contains a collection of physics interfaces that are adapted to a broad category of acoustics simulations in fluids and solids. It supports transient, eigenfrequency, frequency domain, mode analysis, and boundary mode analysis in pressure acoustics in compressible and irrotational velocity fields [6]. In this thesis, the two physics modes used are as follows:

##### **1. Acoustic-Structure Interaction Physics Mode**

This is a multiphysics mode where the fluid’s pressure causes a fluid load on the solid domain, and the structural acceleration affects the fluid domain as a normal acceleration across the fluid-solid boundary. In the frequency domain, the harmonic sound waves in the fluid domain are governed by the Helmholtz equation:

$$\nabla \cdot \left( -\frac{1}{\rho_c} (\nabla p + \mathbf{q}) \right) - \frac{\omega^2 p}{\rho_c c^2} = 0 \quad (22)$$

where the acoustic pressure is  $p = p_0 e^{i\omega t}$  in (N/m<sup>2</sup>) and

- $\rho_c$  : fluid density (kg/m<sup>3</sup>)
- $\mathbf{q}$  : optional dipole source (m/s<sup>2</sup>)
- $\omega$  : angular frequency (rad/s)
- $c$  : speed of sound (m/s)

The default boundary conditions that influence the fluid-solid interaction are the pressure load (force/unit area) by the fluid acting on the solid,

$$\mathbf{F} = -\mathbf{n}_s p \quad (23)$$

where  $\mathbf{n}_s$  is the outward-pointing unit normal vector seen from inside the solid domain, and the normal structural acceleration at the boundary [6],

$$\mathbf{a}_n = \mathbf{n}_s \cdot \mathbf{u}_{tt} \quad (24)$$

where  $\mathbf{u}_{tt}$  is the second derivative of the structural displacement with respect to time.

## 2. Acoustic-Shell Interaction Physics Mode

This mode uses the frequency domain interface feature and a thin shell approximation to model the interactions between a deformable shell and the acoustic pressure in a fluid domain. The shell thickness is defined by the user. The boundary condition to model any deformable shell boundary can be chosen to be an exterior shell or an interior shell. For the exterior shell, only one side of the boundary is adjacent to the fluid domain and the normal acceleration is given by:

$$-\mathbf{n}_s \cdot \left( -\frac{1}{\rho_0} (\nabla p - \mathbf{q}) \right) = \mathbf{n}_s \cdot \mathbf{u}_{tt} \quad (25)$$

and the pressure load on the shell is given by Equation (23).

As for the interior shell, both sides of the boundary interact with the fluid domain. The normal acceleration on each side is akin to Equation (25) and the pressure load on the shell is [6],

$$F_p = -(n_s p)_1 - (n_s p)_2 \quad (26)$$

## B. THE 3D MODEL

A three dimensional model of a thin spherical steel shell was created in COMSOL as shown in Figure 4. The dimension of the thin shell is based on the size of a typical low frequency transducer at  $ka \sim 1$ . As mentioned by Timme, Young and Blue [9, Chp 1], for the case of  $ka < 1$ , the transducer's radiated acoustic power is deemed inefficient. In the present model, the approach to obtain  $ka=1$  is to operate the transducer at 474Hz, which is close to the natural frequency of submerged spherical shell suggested by Junger and Feit [4, Chp 9].

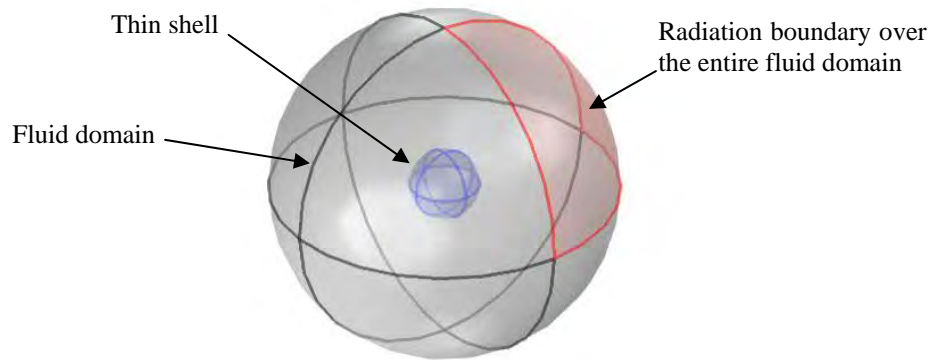


Figure 4. 3D Model of a thin spherical shell submerged in fluid

### 1. Model Parameters

The material of the thin shell is steel and the parameters employed in the model are defined as follows:

$a$	Shell outer radius	0.5m
-----	--------------------	------

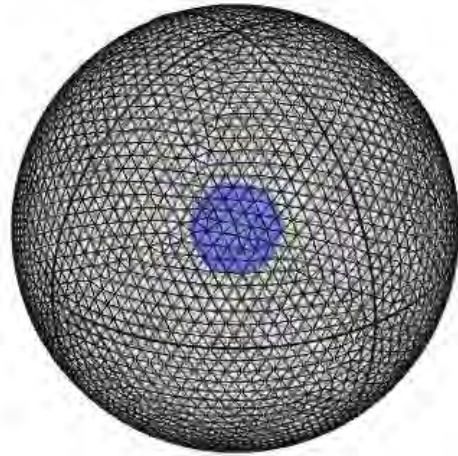
$h$	Shell thickness	0.01m
$R$	Outer radiation boundary of the external fluid	2.5m
$E$	Young's modulus (steel)	215GPa
$\nu$	Poisson's ratio (steel)	0.33
$f$	Operating frequency	474Hz (ka=1)
$\rho_s$	Shell density (steel)	7500kg/m <sup>3</sup>
$\rho_f$	Fluid density	1000kg/m <sup>3</sup>
$C_f$	Sound speed in fluid	1490m/s

## 2. Radiation boundary

A spherical wave radiation boundary condition is specified over the fluid outer boundary to absorb any outgoing waves. Alternatively, a perfectly matched layer (PML) can be used to exhibit the same feature.

## 3. Meshing

Tetrahedral elements were employed to create the mesh. According to COMSOL guideline [6], the mesh element should be no greater than one-fifth of the operating wavelength. For the operating frequency of 474Hz employed, the wavelength in fluid is 3.14m and the maximum element size should be  $\frac{1}{5}\lambda = 0.63\text{m}$  or smaller. The meshed model shown in Figure 5 has a so-called “finer” (COMSOL terminology) mesh for the fluid domain and an “extremely fine” mesh for the thin shell.



**Fluid domain:**

Max element size: 0.175m (0.056  $\lambda$  )

Min element size: 0.0075m (0.0024  $\lambda$  )

**Thin shell:**

Max element size:

0.1m (10 x thickness)

Min element size:

0.001m (0.1 x thickness)

Figure 5. Model with finer mesh for the fluid domain and extremely fine mesh for the thin shell

#### 4. Incident wave onto shell surface

The desired effect is to impose a spherical standing wave acting upon the shell surface as a force per unit area. The equation for the incident pressure was expressed in Equation (2) and is reproduced as Equation (27). As the “Incident pressure” option in COMSOL only acts upon the radiation boundary, the decision was to use the “Background pressure” option to specify the spherical standing wave throughout the volume of the fluid, to achieve the desired effect. The equation of the incident pressure will be elaborated in the next section.

### C. COMSOL MODELING FOR T-MATRIX DETERMINATION

The two important processes for the computation of the T-matrix are specifying the incident standing wave (spherical Bessel functions) and the post evaluation of the scattered pressure (Hankel functions) over the shell surface to obtain the elements of the T-matrix. The workflow of the thin shell modeling in COMSOL is shown in Figure 6.

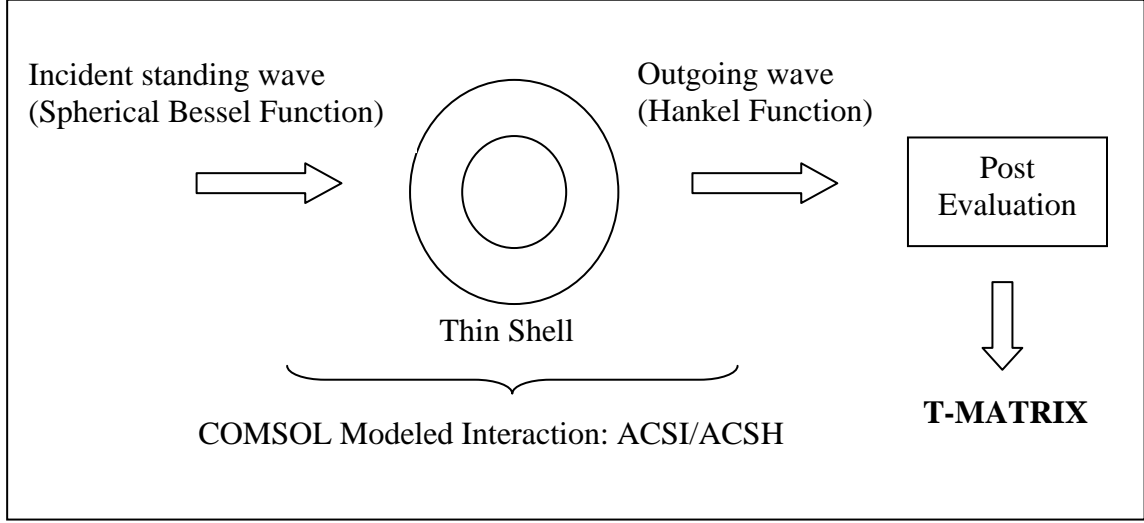


Figure 6. Workflow of COMSOL Modeling

Recall that the incident and scattered waves are taken to be Equations (2) and (3), required here:

$$P^i(r, \theta, \phi) = \sum_{n=0}^{\infty} \sum_{m=-n}^n P_{nm}^i j_n(kr) P_n^m(\cos \theta) e^{im\phi} \quad (27)$$

$$P^s(r, \theta, \phi) = \sum_{n=0}^{\infty} \sum_{m=-n}^n P_{nm}^s h_n^{(2)}(kr) P_n^m(\cos \theta) e^{im\phi} \quad (28)$$

Accounting for scattering up through quadrupolar ( $n=0, 1, 2$ ;  $m=-n, n$ ), the T-matrix between the incident and scattered waves (Equation (1)) takes the following form:

$$\begin{bmatrix} P_{00}^s \\ \vdots \\ P_{22}^s \end{bmatrix} = \begin{bmatrix} R_{00} & \cdots & \cdots & \cdot \\ \vdots & \ddots & & \vdots \\ \vdots & & \ddots & \vdots \\ \cdot & \cdots & \cdots & R_{22} \end{bmatrix} \begin{bmatrix} P_{00}^i \\ \vdots \\ P_{22}^i \end{bmatrix} \quad (29)$$

Each column of the T-matrix is obtained by setting each  $P_{nm}^i$  equal to one, one at a time, while setting all the other  $P_{nm}^i$  to zeros, and employing orthogonality of the spherical harmonics to extract the set of  $P_{nm}^s$  for all  $n$  and  $m$  of interest ( $n=0, 1, 2$ ). For instance, by setting only  $P_{00}^i=1$  and the others to zero, the first column of the T-matrix will be equaled to the corresponding  $P_{nm}^s$  column. The procedure is as follows:

Note, the product  $P_n^m(\cos\theta)e^{im\phi}$  in  $p^i$  and  $p^s$  is related to the usual (normalized) spherical harmonic representation of angular dependence in spherical coordinates by [c.f., 7, Chp 18]

$$Y_n^m(\theta, \phi) = C_{nm} P_n^m(\cos\theta) \exp(im\phi), \quad (30)$$

where

$$C_{nm} = \left\{ (-1)^m \left[ \frac{2n+1}{4\pi} \frac{(n-m)!}{(n+m)!} \right]^{1/2} \right\}. \quad (31)$$

Normalized in this way, the spherical harmonics have the orthonormality property:

$$\int_{-1}^1 \int_0^{2\pi} [Y_n^m(\theta, \phi)]^* Y_{n'}^{m'}(\theta, \phi) d\phi d(\cos\theta) = \delta_{nn'} \delta_{mm'}. \quad (32)$$

In terms of the  $Y_n^m(\theta, \phi)$ , any function of angle can be expanded as [7, Chp 18]:

$$f(\theta, \phi) = \sum_{n=0}^{\infty} \sum_{m=-n}^n a_{nm} Y_n^m(\theta, \phi), \quad (33)$$

where

$$a_{nm} = \int_{-1}^1 \int_0^{2\pi} [Y_n^m(\theta, \phi)]^* f(\theta, \phi) d\phi d(\cos\theta) \equiv C_{nm} I_{nm} \quad (34)$$

and

$$I_{nm} = \int_{-1}^1 \int_0^{2\pi} P_n^m(\cos\theta) \exp(-im\phi) f(\theta, \phi) d\phi d(\cos\theta). \quad (35)$$

Comparing Equations (28) and (33), setting

$$\sum_{n=0}^{\infty} \sum_{m=-n}^n a_{nm} Y_n^m(\theta, \phi) = \sum_{n=0}^{\infty} \sum_{m=-n}^n P_{nm}^s h_n^{(2)}(kr) P_n^m(\cos\theta) e^{im\phi} \quad (36)$$

and eliminating the common terms, the desired expression for scattered pressure amplitude  $P_{nm}^s$  is,

$$P_{nm}^s = \frac{C_{nm} \cdot a_{nm}}{h_n^{(2)}(kr)} = \frac{C_{nm}^2 \cdot I_{nm}}{h_n^{(2)}(kr)}. \quad (37)$$

Equation (37) will be used in the post evaluation of the modeled result  $I_{nm}$ . The required integral, is computed on the shell surface, within COMSOL Multiphysics, using the nodal values of the scattered pressure.

$P_{nm}^s$  is equivalent to the T-matrix element  $R_{nm}$  of spherical harmonics  $n$  and  $m$ . Since the incident pressure amplitudes are always set equal to one, in only one spherical harmonic at a time, the values of  $P_{nm}^s$  so determined are the T-matrix element columnar values.

## IV. RESULTS

This chapter presents the T-matrix elements computed for the specified spherical thin shell, obtained using COMSOL Multiphysics. We consider our goal as to achieve an accuracy of 0.1% for the scattering properties of a single sonar transducer. We base this goal on the supposition that, in a worst case, there might occur as much as 90% destructive interference between elements in an array. Then, if we desire a final array model accuracy of 1% (i.e., 0.1dB), we need an accuracy of 0.1% for the computation of single-element scattering.

For a start, we compute the T-matrix of a rigid sphere in fluid, a less complex model, to examine and become familiar with the functionality of COMSOL. This model was also used to determine the best fluid mesh parameters. We then consider the analysis in using thin shell elements to model the steel shell, to examine the ability and accuracy of the Acoustic-shell Interaction physics mode to model single-element scattering. Finally, we consider the analysis in using true 3D elastic finite elements to model the shell to validate the ability of the Acoustic-structure Interaction physics mode to model the scattering. The T-matrix obtained from each simulation will be verified against an analytical computation of the T-matrix.

In all subsequent calculations of the T-matrix elements, we restrict ourselves to monopolar ( $n=0$ ), dipolar ( $n=1$ ) and quadrupolar ( $n=2$ ) terms. (See Equation (21))

### A. T-MATRIX OF A RIGID SPHERE IN FLUID

The purpose of this section is to examine the functionality of COMSOL by modeling a fluid loaded rigid sphere. This model was simulated in the COMSOL Multiphysics Acoustic-shell Interaction (ACSH) physics mode with the geometry and physical properties listed in Chapter III, Section B, except that the material's density and Young's modulus were increased to  $10^6$  times the original properties, to simulate a rigid, stationary sphere.

As illustrated in Chapter III, Section C, an incident standing wave (spherical Bessel function) as of Equation (27) is imposed onto the object. The scattered pressure (Hankel function) resulted from the interaction is represented by Equation (28). As such, the T-matrix diagonal elements can be determined by evaluating the scattered pressure over the sphere surface using Equation (37).

The analytical T-matrix values for the rigid sphere are presented in Table 1. These were computed using Equation (38), which was evaluated from Equation (20) by taking the limit  $Z_n \rightarrow \infty$ :

$$R_{nm} = -\frac{j'_n(ka)}{h_n^{(2)'}(ka)} = \frac{(n+1)j_{n+1}(ka) - n \cdot j_{n-1}(ka)}{n \cdot h_{n-1}^{(2)}(ka) - (n+1)h_{n+1}^{(2)}(ka)} \quad (38)$$

Table 2 presents two sets of model results, the first obtained using a normal mesh for both the fluid and the solid surface, and the second obtained using more refined meshes for the fluid and solid surface. It only presents the diagonal T-matrix elements; the non-diagonal elements should equal zero and will be considered in a later section.

<b>R<sub>nm</sub></b>	<b>Real part</b>	<b>Imag part</b>	<b>Magnitude</b>	<b>Phase (deg)</b>
R <sub>00</sub>	-4.5351E-02	2.0807E-01	2.1296E-01	1.0230E+02
R <sub>10</sub>	-1.1437E-02	-1.0633E-01	1.0694E-01	-9.6139E+01
R <sub>20</sub>	-1.4876E-04	-1.2196E-02	1.2197E-02	-9.0699E+01

Table 1. Analytical T-matrix for a rigid sphere

Normal mesh for fluid and solid						
$R_{nm}$	Real part	Imag part	Magnitude	Phase (deg)	Mag Error (%)	Phase Error (deg)
$R_{00}$	-4.5050E-02	2.0767E-01	2.1250E-01	1.0224E+02	-0.215	-0.0564
$R_{10}$	-1.1400E-02	-1.0597E-01	1.0658E-01	-9.6140E+01	-0.339	-0.0009
$R_{20}$	-1.4573E-04	-1.2070E-02	1.2071E-02	-9.0692E+01	-1.032	0.0070
Refined Mesh (Fluid: extra fine meshes and solid: extremely fine meshes)						
$R_{nm}$	Real part	Imag part	Magnitude	Phase (deg)	Mag Error (%)	Phase Error (deg)
$R_{00}$	-4.5215E-02	2.0779E-01	2.1265E-01	1.0228E+02	-0.142	-0.0199
$R_{10}$	-1.1413E-02	-1.0620E-01	1.0681E-01	-9.6134E+01	-0.123	0.0053
$R_{20}$	-1.4686E-04	-1.2155E-02	1.2156E-02	-9.0692E+01	-0.335	0.0066

Table 2. COMSOL: T-matrix for a rigid sphere

The T-matrix elements for the rigid sphere were evaluated on the sphere surface. For the normal mesh, the element size is:

**Fluid:**

Maximum element size = 0.5 m ( $0.16\lambda$ )

**Sphere surface:**

Maximum element size = 0.2 m ( $0.064\lambda$ )

As for the refined mesh, the element size is:

**Fluid (extra fine mesh):**

Maximum element size = 0.175 m ( $0.056\lambda$ )

**Sphere surface (extremely fine mesh):**

Maximum element size = 0.1 m ( $0.032\lambda$ )

From Table 2, quadrupole  $R_{20}$  is observed to be the worst case, with the highest magnitude error. After a refined mesh was introduced, its magnitude error with respect to the analytical values shows an improvement from -1.032% to -0.335%. In view of the goal of 0.1% accuracy, these results are considered marginally satisfactory.

## B. T-MATRIX OF A THIN SPHERICAL SHELL USING THIN SHELL APPROXIMATION

### 1. Analytical T-matrix

The analytical values are determined by Equation (20) using thin shell approximation. The T-matrix diagonal elements are shown in Table 3.

$R_{nm}$	Real part	Imag part	Magnitude	Phase (deg)
$R_{00}$	-1.3696E-02	1.1623E-01	1.1703E-01	9.6721E+01
$R_{10}$	-6.0902E-03	7.7802E-02	7.8039E-02	9.4476E+01
$R_{20}$	-6.2949E-04	-2.5082E-02	2.5090E-02	-9.1438E+01

Table 3. Analytical T-matrix for a thin shell at  $n=0, 1$  and  $2$

### 2. COMSOL Results for Thin Shell Approximation Modeling

#### a. Diagonal elements of T-matrix

The thin spherical shell was modeled in the COMSOL Multiphysics Acoustic-shell Interaction (ACSH) physics mode with extra fine meshes for the fluid domain and extremely fine meshes for the shell surface. In this mode, the shell is modeled using thin shell finite elements, that is, the shell is modeled with a thin shell approximation [4, Chp 7]. The mesh element sizes are similar to the refined mesh of the rigid sphere in previous section.

The mesh of the model consisted of 214299 elements and 298606 degrees of freedom (DOF). It was computed over an average time frame of 12 minutes. The diagonal T-matrix elements for this model, evaluated on the shell surface, are presented in Table 4. The last two columns show the magnitude and phase errors relative to the analytical T-matrix.

$R_{nm}$	Real part	Imag part	Magnitude	Phase (deg)	Mag Error (%)	Phase Error (deg)
$R_{00}$	-1.3693E-02	1.1623E-01	1.1703E-01	9.6719E+01	0.0010	-0.0019
$R_{1,-1}$	-6.0884E-03	7.7799E-02	7.8037E-02	9.4475E+01	-0.0027	-0.0012
$R_{10}$	-6.0831E-03	7.7767E-02	7.8004E-02	9.4473E+01	-0.0449	-0.0032
$R_{11}$	-6.0884E-03	7.7799E-02	7.8037E-02	9.4475E+01	-0.0027	-0.0012
$R_{2,-2}$	-6.2334E-04	-2.5011E-02	2.5019E-02	-9.1428E+01	-0.2818	0.0100
$R_{2,-1}$	-6.2475E-04	-2.5039E-02	2.5047E-02	-9.1429E+01	-0.1706	0.0084
$R_{20}$	-6.2540E-04	-2.5053E-02	2.5061E-02	-9.1430E+01	-0.1133	0.0077
$R_{21}$	-6.2475E-04	-2.5039E-02	2.5047E-02	-9.1429E+01	-0.1706	0.0084
$R_{22}$	-6.2335E-04	-2.5011E-02	2.5019E-02	-9.1428E+01	-0.2818	0.0100

Table 4. COMSOL: Diagonal T-matrix elements for a thin shell (fluid domain: extra fine meshes and shell surface: extremely fine meshes)

From the results presented in Table 4, three observations were made. Firstly, the magnitude error for  $R_{00}$ ,  $R_{10}$  and  $R_{20}$ , ascertained that the results are in better agreement than those of the rigid sphere. The discrepancy is unknown at this juncture and remains to be investigated.

The second observation deduced that the results are almost independent of the azimuthal mode number,  $m$ , as they should be for the case of an axisymmetric scatterer. However, for the modeling in COMSOL, the axisymmetric characteristics could have been slightly affected by the differing mesh sizes built on the model.

The third observation arises from the comparison with the T-matrix determined by ATILA Finite-Element Modeling, with its results presented in Table 5 [2, Chp 3]. The model was composed of 2746 nodes and 288 mesh elements. The number of mesh elements is nearly a thousand times lesser than the COMSOL mesh elements of 214299. It can be seen from the last two columns that a high magnitude error of up to -38% occurred in the quadrupole scattering computation. It is, therefore, evident that a mesh refinement in COMSOL modeling has yielded more accurate results.

$R_{nm}$	Real part	Imag part	Magnitude	Phase (deg)	Mag Error (%)	Phase Error (deg)
$R_{00}$	-1.2624E-02	1.1429E-01	1.1499E-01	9.6303E+01	-0.91	-0.36
$R_{1,-1}$	-6.8902E-03	8.2376E-02	8.2664E-02	9.4781E+01	6.49	0.33
$R_{10}$	-5.7422E-03	8.3113E-02	8.3311E-02	9.3952E+01	7.33	-0.50
$R_{11}$	-6.8668E-03	8.2363E-02	8.2649E-02	9.4766E+01	6.47	0.31
$R_{2,-2}$	-2.8487E-03	-1.5203E-02	1.5468E-02	-1.0061E+02	-37.8	-9.19
$R_{2,-1}$	-2.7899E-03	-1.5159E-02	1.5414E-02	-1.0043E+02	-38.0	-9.00
$R_{20}$	-2.4889E-03	-1.5287E-02	1.5488E-02	-9.9247E+01	-37.7	-7.82
$R_{21}$	-2.7847E-03	-1.5164E-02	1.5418E-02	-1.0041E+02	-38.0	-8.98
$R_{22}$	-2.8227E-03	-1.5182E-02	1.5442E-02	-1.0053E+02	-37.9	-9.11

Table 5. ATILA: Diagonal T-matrix elements for a thin shell [2, Chp 3]

***b. Non-diagonal elements of T-matrix***

The non-diagonal element is a measure of the T-matrix efficacy. A significant value indicates an existence of a numerical “leakage” in the model computation. In the T-matrix determined by ATILA, there are two significant leakages [2, Chp 4].

The T-matrix in Table 6 presents the non-diagonal elements relative to the diagonal elements in the same column. This normalization was chosen because the T-matrix elements are computed one column at a time. For instance, the non-diagonal value for  $R_{10}$  (third column) relative to  $R_{00}$  (first row) corresponds to  $4.98E-5$ .

The largest three non-diagonal values are  $1.63E-03$  (monopole to dipole),  $1.63E-03$  (dipole to quadrupole) and  $1.16E-02$  (quadrupole to quadrupole), as highlighted in Table 6. However, these values are not considered to be significantly causing a leakage in the model. As a comparison to ATILA modeling, the reduction in leakage could have been due to the finer mesh employed in the COMSOL modeling.

		Incident Pressure								
		$R_{00}$	$R_{1,-1}$	$R_{10}$	$R_{11}$	$R_{2,-2}$	$R_{2,-1}$	$R_{20}$	$R_{21}$	$R_{22}$
Scattered Pressure	$R_{00}$	1	1.80E-04	4.98E-05	3.61E-04	4.76E-07	6.34E-06	5.78E-05	4.24E-05	1.32E-05
	$R_{1,-1}$	1.63E-03	1	6.16E-05	2.40E-05	6.77E-07	8.13E-06	3.14E-04	2.22E-05	9.27E-06
	$R_{10}$	2.41E-04	3.07E-05	1	6.19E-05	1.61E-06	1.40E-05	5.98E-05	8.05E-05	3.91E-05
	$R_{11}$	8.15E-04	6.04E-06	3.05E-05	1	1.51E-07	1.83E-06	1.56E-04	2.42E-05	1.10E-05
	$R_{2,-2}$	2.79E-04	1.34E-04	1.80E-04	6.88E-05	1	3.67E-05	8.61E-05	3.70E-04	1.16E-02
	$R_{2,-1}$	8.54E-04	1.34E-04	4.48E-04	1.60E-04	9.16E-06	1	2.08E-04	4.62E-04	3.70E-04
	$R_{20}$	7.85E-04	8.13E-04	2.19E-04	1.63E-03	3.60E-06	3.46E-05	1	2.08E-04	8.59E-05
	$R_{21}$	1.42E-04	1.35E-05	7.64E-05	4.43E-05	2.56E-06	1.28E-05	3.46E-05	1	3.67E-05
	$R_{22}$	1.11E-05	1.44E-06	7.48E-06	1.11E-05	2.01E-05	2.56E-06	3.61E-06	9.16E-06	1

Table 6. Non-diagonal elements in the T-matrix normalized to diagonal element in the same column (Thin shell approximation)

*c. Evaluation of T-matrix within fluid (at radius = 1m and 2m)*

An important issue is to ascertain the best position to evaluate the T-matrix, that is, on the shell surface or at some distance into the fluid. To investigate this, the T-matrix diagonal elements were computed at surfaces within the fluid, at radii of 1 meter and 2 meters, respectively. The T-matrix elements determined by COMSOL are presented in Table 7, with the errors shown in the last two columns:

At radius=1m						
$R_{nm}$	Real part	Imag part	Magnitude	Phase (deg)	Mag Error (%)	Phase Error (deg)
$R_{00}$	-1.3698E-02	1.1624E-01	1.1704E-01	9.6721E+01	0.0078	0.0002
$R_{10}$	-6.0761E-03	7.7731E-02	7.7968E-02	9.4470E+01	-0.0916	-0.0063
$R_{20}$	-6.2362E-04	-2.5007E-02	2.5014E-02	-9.1429E+01	-0.2994	0.0092
At radius=2m						
$R_{nm}$	Real part	Imag part	Magnitude	Phase (deg)	Mag Error (%)	Phase Error (deg)
$R_{00}$	-1.3699E-02	1.1624E-01	1.1704E-01	9.6722E+01	0.0077	0.0009
$R_{10}$	-6.0763E-03	7.7731E-02	7.7969E-02	9.4470E+01	-0.0908	-0.0062
$R_{20}$	-6.2379E-04	-2.5012E-02	2.5020E-02	-9.1429E+01	-0.2784	0.0091

Table 7. COMSOL: Diagonal T-matrix elements at radius = 1m and 2m respectively (fluid domain: extra fine meshes and shell surface: extremely fine meshes)

Comparing to the T-matrix evaluated on the shell surface in Table 4, the magnitude errors for  $R_{00}$ ,  $R_{10}$  and  $R_{20}$  were 0.001%, -0.0449% and -0.1133% respectively. This has obviously shown that the T-matrix evaluated on the shell surface yields a more accurate result.

**C. T-MATRIX OF A THIN SPHERICAL SHELL USING 3D ELASTIC THEORY**

From the results of the rigid sphere scattering and using thin shell approximation for the shell, we have developed good confidence in COMSOL modeling. The next important step is to verify whether the thin shell approximation is able to exhibit the realistic behavior of a true 3D elastic shell. This involves the use of the 3D elastic theory

to compute the T-matrix of a fluid-loaded thin shell. The COMSOL Multiphysics Acoustic-Structure Interaction (ACSI) physics mode is capable of performing such simulation to achieve accurate values of the T-matrix.

## 1. Analytical T-matrix

The analytical T-matrix was determined based on the 3D elastic theory and the formulation procedures suggested by Hickling [10]. The T-matrix diagonal elements are shown in Table 8. The last two columns show the magnitude error percentage in the analytical T-matrix using thin shell approximation, relative to that of the 3D elastic theory. The analytical T-matrix using thin shell approximation can be found in Table 3.

$R_{nm}$	Real part	Imag part	Magnitude	Phase (deg)	Thin shell Mag Error (%)	Thin shell Phase Error (deg)
$R_{00}$	-1.4191E-02	1.1828E-01	1.1913E-01	9.6842E+01	-1.76	-0.12
$R_{10}$	-6.3614E-03	7.9504E-02	7.9758E-02	9.4575E+01	-2.15	-0.10
$R_{20}$	-6.2112E-04	-2.4915E-02	2.4923E-02	-9.1428E+01	0.67	-0.01

Table 8. Analytical T-matrix for a thin shell using 3D elastic theory

From the magnitude error shown in Table 8, it is obvious that the thin shell approximation has a discrepancy in accuracy of up to 2%, relative to the 3D elastic theory. Hence, it is important to note that computations based on the thin shell approximation theory are not sufficiently accurate to exhibit the real behavior of a 3D element.

## 2. COMSOL Results for 3D Elastic Shell Modeling

### a. Diagonal elements of T-matrix

A full 3D elastic steel shell model was created in the COMSOL Multiphysics Acoustic-Structure Interaction (ACSI) physics mode. A finer mesh was built on the fluid domain and a coarser mesh for the solid domain - the entire thickness of the shell. The element size is as follows:

**Fluid (finer mesh):**

Maximum element size = 0.275 m (0.088 $\lambda$ )

**Shell (coarser mesh):**

Maximum element size = 0.95 m (95 x thickness)

The mesh of the model consisted of 164537 elements and is computed with 318398 degrees of freedom (DOF). It was computed over an average time frame of 7 minutes.

The diagonal T-matrix elements employing the 3D elastic theory, evaluated on the shell surface, are presented in Table 9. The last two columns show the magnitude and phase errors relative to the analytical T-matrix.

$R_{nm}$	Real part	Imag part	Magnitude	Phase (deg)	Mag Error (%)	Phase Error (deg)
$R_{00}$	-1.4187E-02	1.1828E-01	1.1912E-01	9.6840E+01	-0.0031	-0.0019
$R_{1,-1}$	-6.3584E-03	7.9489E-02	7.9743E-02	9.4573E+01	-0.0185	-0.0013
$R_{10}$	-6.3584E-03	7.9489E-02	7.9743E-02	9.4573E+01	-0.0188	-0.0013
$R_{11}$	-6.3584E-03	7.9489E-02	7.9743E-02	9.4573E+01	-0.0185	-0.0013
$R_{2,-2}$	-6.1726E-04	-2.4896E-02	2.4904E-02	-9.1420E+01	-0.0766	0.0078
$R_{2,-1}$	-6.1720E-04	-2.4895E-02	2.4903E-02	-9.1420E+01	-0.0802	0.0079
$R_{20}$	-6.1723E-04	-2.4896E-02	2.4903E-02	-9.1420E+01	-0.0779	0.0078
$R_{21}$	-6.1720E-04	-2.4895E-02	2.4903E-02	-9.1420E+01	-0.0802	0.0079
$R_{22}$	-6.1726E-04	-2.4896E-02	2.4904E-02	-9.1420E+01	-0.0766	0.0078

Table 9. COMSOL: Diagonal T-matrix elements for a thin shell using 3D elastic theory (fluid domain: finer meshes and shell: coarser meshes)

An overview of the magnitude errors in Table 9 shows that the T-matrix determined by COMSOL using the 3D elastic theory is in excellent agreement with the analytical T-matrix. It has also shown that the T-matrix is independent of the azimuthal mode number,  $m$ .

It was noted that the mesh of the 3D elastic model was not as refined as the thin shell approximation model. Hence, a further step was taken to examine if a mesh

refinement will improve the results of the 3D elastic model. A test case on  $R_{00}$ , built with finer meshes for both the fluid and solid domain was created. The computation time was 2.5 hours and the results are presented in Table 10.

$R_{nm}$	Real part	Imag part	Magnitude	Phase (deg)	Mag Error (%)	Phase Error (deg)
$R_{00}$	-1.4181E-02	1.1825E-01	1.1910E-01	9.6838E+01	-0.0237	-0.0032

Table 10. Improved meshing for computing  $R_{00}$  using 3D elastic theory (fluid: finer meshes and solid: finer meshes)

The results in Table 10 show that the magnitude error for  $R_{00}$  increases despite the mesh refinement. It has proven that mesh refinement may not necessarily be the improvement factor to achieve accuracy. The reason, however, is unclear at this juncture and further investigation will be required.

***b. Non-diagonal elements of  $T$ -matrix***

The non-diagonal elements relative to the diagonal elements for the full 3D elastic model are presented in Table 11. The largest three values are 1.80E-03 (monopole to quadrupole), 1.13E-03 (monopole to quadrupole) and 1.11E-03 (quadrupole to quadrupole). These values will not cause a significant leakage in the model. Comparatively, these non-diagonal values are lower than that of the thin shell approximation model. As the full 3D elastic shell model has a “real” thickness that enables mesh to be built on, the computation is definitely more precise than the model based on thin shell approximation.

		Incident Pressure								
		$R_{00}$	$R_{1,-1}$	$R_{10}$	$R_{11}$	$R_{2,-2}$	$R_{2,-1}$	$R_{20}$	$R_{21}$	$R_{22}$
Scattered Pressure	$R_{00}$	1	2.19E-05	2.95E-05	4.38E-05	2.85E-06	8.02E-06	2.42E-06	4.63E-05	7.92E-05
	$R_{1,-1}$	1.99E-04	1	2.37E-05	3.50E-05	1.45E-05	2.33E-05	2.21E-05	7.10E-05	1.09E-04
	$R_{10}$	1.32E-04	1.17E-05	1	2.37E-05	2.97E-06	1.76E-05	2.14E-05	1.06E-04	7.12E-05
	$R_{11}$	9.95E-05	8.95E-06	1.17E-05	1	2.25E-06	5.90E-06	1.11E-05	6.99E-05	1.73E-04
	$R_{2,-2}$	1.80E-03	7.69E-04	3.90E-04	6.10E-04	1	2.87E-04	5.86E-04	6.62E-04	1.11E-03
	$R_{2,-1}$	1.13E-03	3.68E-04	4.87E-04	3.81E-04	7.17E-05	1	2.09E-04	4.45E-04	6.62E-04
	$R_{20}$	3.05E-05	4.46E-05	1.13E-04	8.92E-05	2.45E-05	3.49E-05	1	2.09E-04	5.86E-04
	$R_{21}$	1.90E-04	3.16E-05	8.10E-05	1.23E-04	4.59E-06	1.24E-05	3.49E-05	1	2.87E-04
	$R_{22}$	7.51E-05	1.27E-05	1.61E-05	6.39E-05	1.93E-06	4.59E-06	2.45E-05	7.17E-05	1

Table 11. Non-diagonal elements in the T-matrix normalized to diagonal element in the same column (3D Elastic Theory)

## V. CONCLUSIONS AND FUTURE WORK

### A. CONCLUSIONS

The T-matrix of a fluid-loaded thin spherical steel shell of radius  $a$ , has been calculated using the COMSOL Multiphysics Finite-Element Code for  $ka=1$  (where  $k$  is the acoustic wave number). In order to observe the behavior at  $ka=1$ , the thin shell radius was chosen to be 0.5m, with a thickness of 1cm, and driven at a frequency of 474Hz. The goal of attaining a result accuracy of 0.1% relative to the analytical T-matrix was achieved in a model employing 3D elastic finite elements.

The modeling process was structured into three progressions. The starting point was to compute the T-matrix of a fluid-loaded rigid sphere using the Acoustic-Shell Interaction (ACSH) physics mode to examine the functionality of the COMSOL Multiphysics code. Secondly, using the same physics mode ACSH, the T-matrix of a fluid-loaded thin spherical shell was determined by employing the thin shell approximation theory. Lastly, the T-matrix of a true elastic shell was determined by adopting the 3D elastic theory using the Acoustic-Structure Interaction (ACSI) physics mode.

The T-matrix elements for the rigid sphere, evaluated on the sphere surface, were found to be marginally satisfactory relative to the analytical values. The quadrupole,  $R_{20}$  was observed to be the worst case with the highest magnitude error. The magnitude error with respect to the analytical values showed an improvement from -1.032% to -0.335% when a mesh refinement of the fluid and solid domain was introduced.

In the evaluation of the T-matrix on the shell surface using thin shell approximation theory, the results appeared to be in better agreement than those of the rigid sphere. The T-matrix magnitude error were ranged from -0.28% to 0.001%, relative to the analytical values for a thin shell. The non-diagonal elements had shown that there was no significant “leakage” in the model. Also, the T-matrix was evaluated at two radii

(1meter and 2meters) within the fluid. The results determined were not as favorable as those evaluated on the shell surface.

In modeling the thin shell as a true 3D elastic element, the simulation based on the 3D elastic theory was able to achieve the goal of attaining an accuracy of at least 0.1%. The model was computed using the Acoustic-Structure Interaction (ACSI) physics mode and the T-matrix was evaluated on the shell surface. The resulting average magnitude error was less than 0.08%, relative to the analytical values. Also, the non-diagonal values were not significant.

The COMSOL Multiphysics Finite-Element Code has proven its ability to model the scattering of acoustic waves from a thin shell. Comparing the T-matrix results obtained by ATILA in the previous attempt, COMSOL is superior in terms of efficiency and accuracy.

## **B. FUTURE WORK**

In spite of the satisfying results obtained in COMSOL Multiphysics Finite-Element Code, there are three areas that can be explored to further improve the results accuracy.

### **1. External determination of scattering coefficients**

It is unclear about the preciseness of the post evaluation performed by COMSOL which can possibly introduce small numerical errors. It can, therefore, be investigated by performing an external determination of the scattering coefficients by an alternate program such as MATLAB. In this case, the nodal values obtained in COMSOL will have to be exported to MATLAB in which a singular value decomposition using Equation (28) can be performed by the least square curve-fitting procedures.

### **2. Perform swept mesh in radial direction**

Since a refined mesh may not be necessary for the entire domain, for instance, the fluid domain, the swept mesh technique can be explored. The swept mesh allows different refinement on a surface. With this option, the user will be able to specify the

essential size of the mesh and sweep radially within the domain. In this case, the computing resource can be preserved.

### **3. Perfectly Matched Layer (PML)**

The absorption of outgoing waves can be investigated by replacing the radiation boundary condition at the fluid outer radius by a perfectly matched layer (PML) to observe the difference in wave scattering amplitudes. A PML may perform better in terms of absorbing outgoing radiation when the scatterer is not spherical. This remains to be investigated.

THIS PAGE INTENTIONALLY LEFT BLANK

## LIST OF REFERENCES

- [1] C. L. Scandrett and S. R. Baker, “*T-matrix Approach to Array Modeling*,” Naval Postgraduate School, Monterey, CA, 1998.
- [2] Ruiz, Arthur L. D., “*Calculation of the Transition Matrix for the Scattering of Acoustic Waves From a Thin Elastic Spherical Shell Using The ATILA Finite Element Code*,” Master’s Thesis, Naval Postgraduate School, Monterey, CA, 1994.
- [3] C. L. Scandrett and D. R. Canright, “*Acoustic Interactions in Arrays of Spherical Elastic Shells*,” *Journal of Acoustic Society of America*, Vol. 90, pp. 589-595, July 1991.
- [4] Junger, M. C. and Feit, D., “*Sound, Structures, and Their Interaction*,” 2<sup>nd</sup> edition, Massachusetts Institute of Technology, 1986.
- [5] Weisstein, Eric W, “*Spherical Coordinates*,” MathWorld – A Wolfram Web Resource. <http://mathworld.wolfram.com/SphericalCoordinates.html> (accessed 2 Oct, 2011)
- [6] COMSOL Multiphysics, “*Acoustics Module User Guide Version 4.2*,” User’s Manual, May 2011.
- [7] K. F. Riley, M. P. Hobson, and S. J. Bence, “*Mathematical Methods for Physics and Engineering*,” Cambridge University Press, New York, Third edition, 2006.
- [8] L. E. Kinsler, A. R. Frey, A. B. Coppens, and J. V. Sanders, “*Fundamentals of Acoustics*,” John Wiley & Sons, Inc., Fourth edition, 2000.
- [9] B. F. Hamonic, O. B. Wilson, J.-N. Decarpigny, eds., “*Power Transducers for Sonics and Ultrasonics*,” Proceedings of the International Workshop held in Toulon, France, June 12 and 13, 1990.
- [10] Robert Hickling, “*Analysis of Echoes from a Hollow Metallic Sphere in Water*,” *Journal of Acoustic Society of America*, Vol. 36, Number 6, June 1964.

THIS PAGE INTENTIONALLY LEFT BLANK

## INITIAL DISTRIBUTION LIST

1. Defense Technical Information Center  
Ft. Belvoir, Virginia
2. Dudley Knox Library  
Naval Postgraduate School  
Monterey, California
3. Professor Andres Larraza  
Code PH/La  
Naval Postgraduate School  
Monterey, California
4. Professor Steve Baker  
Code PH/Ba  
Naval Postgraduate School  
Monterey, California
5. Professor Clyde L. Scandrett  
Code MA/Sd  
Naval Postgraduate School  
Monterey, California
6. Professor Yeo Tat Soon  
Director, Temasek Defence Science Institute  
National University of Singapore  
Singapore
7. Tan Lai Poh (Ms)  
Senior Manager, Temasek Defence Science Institute  
National University of Singapore  
Singapore
8. Ng Kiang Chuan  
Ministry of Defence  
Singapore